**Investigation of the Properties of Magnetic
Films Deposited on Carbon Nitride**

A thesis submitted in partial fulfillment of the requirement
for the degree of Bachelor of Science with Honors in
Physics from the College of William and Mary in Virginia,

by

Travis L. Turner

Accepted for

_____

(Honors, High Honors, or Highest Honors)

_____

Director

Dr. Anne Reilly

_____

_____

_____

Williamsburg, Virginia
April 2001

Table of Contents

3

Acknowledgements

I would like to thank Dr. Anne Reilly for her support and enthusiasm for my project. Additionally, I like to thank Dr. Brian Holloway for the use of his laboratory. Data collection could not have taken place without the assistance of Amy Wilkerson (ARC) and Dr. Buzz Wincheski (NASA Langley). Jason Gammon produced all of the CN layers used in the study. Special thanks goes to my summer lab partner Jeff Groff, who gave the project a tremendous boost. Last, but not least, I would also like to thank all of the kind faculty and students of the physics department.

Abstract

The purpose of this study is to investigate the magnetic and structural properties of nickel films when deposited on hard and amorphous carbon thin films. We are interested in both magnetic properties related to the giant magnetoresistive effect, such as saturation magnetization and field coercivity and changes in roughness of the films. These films were also annealed to determine whether or not temperature would affect them greatly. Since each film must be heated in order to deposit another layer of carbon to produce a multilayer film, we must discover what these changes are and how they influence the above properties.

I . Introduction

Giant magnetoresistance (GMR) is defined as the relative change in electrical resistance ($\Delta R/R$) seen in ferromagnetic/non-magnetic multilayer thin films when a magnetic field is applied. This is a new and quickly growing discipline; the original paper in 1988 noted a 100%[1] change in resistance and the record was a 220% change by 1995[2]. GMR multilayers are constructed of alternating ferromagnetic (e.g. Co) and non-magnetic materials (e.g. Cu) with layers that are only tens of nanometers thick. The source of GMR is spin–dependent electron transport in the layers. Because GMR multilayers react strongly to a changing magnetic field, they can be used to sense these fields. This has led to the important application of sensors in the computer industry. In hard drive read heads, GMR materials are able to sense small changes in

external magnetic fields because of large changes in the sensor's resistivity. Since IBM first used GMR sensors in the later part of the 1990's[3], we have seen incredible increases in hard drive capacities, with more advances to come.

Because of the many different properties of carbon, it is of interest to consider incorporating it into the multilayers of GMR and spin-dependent tunneling films. It can be an excellent insulator and very durable, as in the case of diamond, or it can be a soft conductor, as in graphite. Hard carbon films might represent an improvement over the materials currently in use, such as Al_2O_3. One advantage is that the properties of the carbon layers can be fine tuned by changing the deposition conditions. In particular the resistivity could be manipulated for use in high impedance devices, such as storage media, or low impedance devices used for sensors. Our research concerns itself with hard carbon films, especially amorphous carbon nitride (CN), which we are exploring for possible use as the insulating layer within a thin film device. This field is relatively new and definitely exciting; as of yet most applications of hard carbon involving these devices are as a coating for magnetic media. With the ability to manipulate the before-mentioned properties, perhaps amorphous carbon might replace the oxides currently used as the insulating layer in these devices.

In this study we produced ferromagnetic films of nickel on carbon nitride thin films by sputtering, using silicon as a substrate. Magnetic properties and roughness were examined to determine if carbon nitride could be incorporated into a GMR multilayer without negatively impacting the magnetic and electrical

properties. To promote good film growth for the carbon nitride layer, we must heat the substrate to temperatures possibly as high as 600° C. Therefore, a thorough understanding of the effect on the magnetic and physical properties of these preliminary films is required in order to proceed with our production of more useful samples.

II. Theory

A. Magnetic Properties

A material is constructed of atoms, each with a magnetic moment. These magnetic moments come from three sources, the atom's orbital angular momentum, the electron spin, and the change in the orbital moment induced by an applied magnetic field. When the field is applied, these magnetic moments tend to either align themselves with the applied field, which is called paramagnetism, or to align in the opposite direction, as in diamagnetism. This alignment of magnetic dipoles causes a net polarization—in short another magnet is created. When a material retains this polarization after the magnetic field is removed, then it is said to be ferromagnetic.

The familiar Lenz's law in electrodynamics easily explains diamagnetism. Simply put, Lenz's law states that nature opposes a change in flux. In the presence of a magnetic field there will exist a finite current around the nucleus. In turn, this current produces a magnetic field opposite to that of the external field. In paramagnetism, when atoms have magnetic moments that interact very weakly with each other, they tend to align themselves with the external field in

order to minimize energy.

Ferromagnets result from a much stronger interaction between the spin of one atom and that of another close by it. The Heisenberg model provides a simple description of the energy of interaction, or the exchange energy.

$$U = -2J\mathbf{S}_1 \cdot \mathbf{S}_2 \qquad (1)$$

J is called the exchange integral and is closely related to the distribution of charge between atoms i and j. In cobalt, nickel, and iron, for example, J is positive. In these cases, the two spins must align in order to minimize energy. In an applied field, the magnetic dipole moments work to align themselves with the field, as in a paramagnetic material. The system will prefer a state that minimizes the energy and in the case where J is positive, this requirement aligns the spins and consequently the magnetic moments in the same direction. When the field is removed the material will remain magnetized in order to minimize energy. At the Curie Temperature (which is specific to the material) the thermal energy of the atoms in a ferromagnet is sufficient to misalign the magnetic moments and cause the sample to lose its magnetization

As found in nature, ferromagnetic materials do not have a large net polarization. Instead, there are regions in which magnetic moments are arranged in the same direction, called domains. The separations between these domains are called domain walls. The domain structure also results from a need for the system to minimize energy. Energy is stored in the total magnetic

field so to minimize it the dipoles align themselves with each other to cancel the

magnetic fields of adjacent domains.   As an external magnetic field is applied

the number of walls shrink, until a single domain forms. When the applied field

is removed, the number of domains increases until the energy to produce a new

wall is no longer less than the energy stored in the surrounding fields.

It is this domain wall motion that gives use to hysteresis in the magnetization, as

shown in Figure 1.

Figure 1 – A Typical Hysteresis Loop

First magnetization will reach point of saturation. The magnetization reaches
saturation, applied field is decreased and magnetization decreases. Negation
Saturation Magnetization is reached.   As applied field increases the loop
raises to positive saturation once more
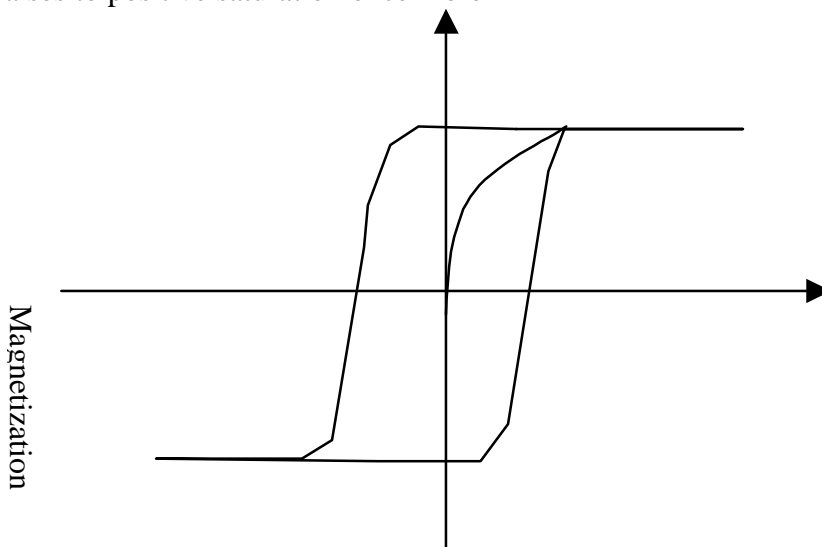
To study the graph more carefully several terms must be defined.   The

distance spanned by the curve on the x-axis is called the coercivity and the field

needed to bring the magnetization to zero is called the coercive force.   The

lesser the coercivity the more sensitive the specimen is to changes in the

applied field. When the hysteresis loop begins to flatten a condition called saturation has been reached with only one domain. At saturation the value of the magnetization is at a maximum called the saturation magnetization. As mentioned, domain motion mainly determines the shape of the hysteresis loop, and is very sensitive to the structural properties of the film. Therefore, to produce films with the lowest coercivity and highest saturation magnetization (a must for sensors), thin films must be made smooth and with the lowest number of defects as possible.

B. Giant Magnetoresistance

The GMR effect can be observed in ferromagnetic / non-magnetic multilayers. These films will sometimes spontaneously orient their magnetization in an antiparallel configuration (AP) where by each layer has a magnetization, which alternates by 180 degrees throughout the film. (Figure 2). This occurs through magnetic interaction between the ferromagnetic layers.

Figure 2 – Antiparallel Configuration. The electrons (shaded arrows) pass through the highly resistive film. F represents a ferromagnetic layer, N is non-ferromagnetic layer.
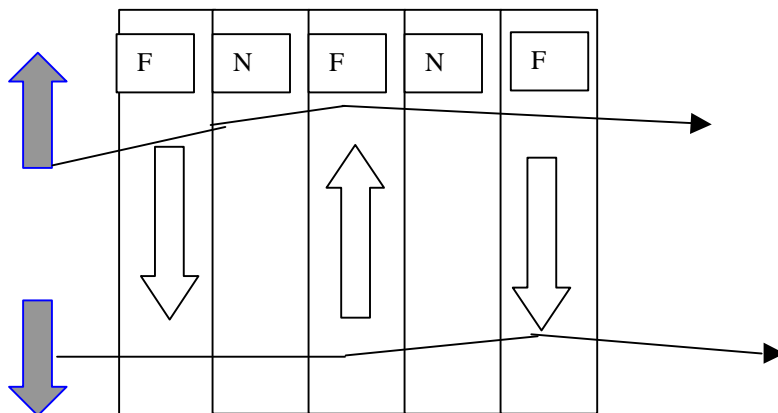
When a magnetic field is applied, the layers begin to align their magnetizations with the field creating a parallel (P) configuration (Figure 3). There is a difference in resistance of the multilayer for these two configurations because of the fact that scattering rates, and thus resistivity are dependent on the spin (½ or -½) of the electron. For an electron moving through a layer with the same spin as the magnetization in that layer, nearly all available quantum states are full (known as the majority state). Conversely, for an electron of opposite spin moving through the same layer, the states available to it are partially filled (minority states). Scattering is dependent on the availability of states into which an electron can scatter, so an electron in the minority state scatters more. The opposite is true of electrons in the majority state. In the AP configuration, electrons can scatter through the magnetic layers of the film just as easily with either a spin of ½ or -½ In the P case, electrons with parallel spins are in the majority state, thus, they scatter less, resulting in a lower resistance for electrons in that state, (see Figure 3). The net effect is called spin polarization, where the film will allow far more electrons from one spin state to pass through than another.   The act of these spin-polarized electrons moving through the film is known as spin dependent transport and causes the large increases in resistance found in GMR materials when they are subjected to a magnetic field.

Figure 3 – Parallel Configuration. The electrons (shaded arrows) pass through the multilayer film. Those in one state are favored, and pass easily through the material.
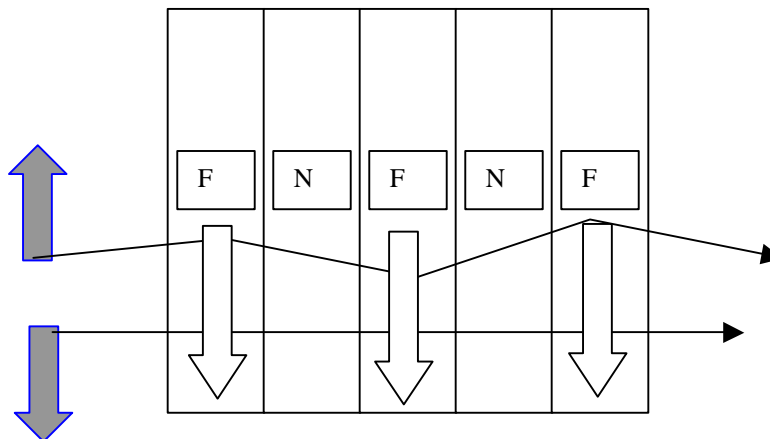
C. Dependence of Magnetic and Transport Behavior on Structural Properties

The magnetic properties of the film can be greatly affected by its structural properties. Saturation magnetization may decrease if any unwanted chemical compound forms during the sputtering process, or if there is intermixing between layers at the interface (e.g., Ni and C interact to form nickel carbide, which has a much lower magnetization). Defects in the film tend to increase the coercivity of the hysteresis loops since the domain walls become "hung" on the defects and impurities in the film, making it much more difficult for a single domain to form. Therefore, it takes a greater applied field to produce a similar effect in a sample containing impurities and defects, limiting the films usefulness as a GMR sensor. The roughness of the surface at each interface can also change the magnetic properties. The rougher the transition between layers the

greater the diffuse scattering of electrons. This lowers the chances of a strong

GMR effect.

D. Sputtering

Over a hundred years ago a process now known as cathode sputtering

was developed[11]. The most common setup involves placing the material to be

sputtered at the cathode, which is kept at a negative high voltage. A substrate

of silicon rests on the anode, which may be at ground. These two are separated

by a distance denoted "d" on the diagram below. The process takes place within

the confines of a vacuum chamber in a low pressure of argon gas. (See Figure

4)

Figure 4 – The Setup. A typical cathode sputtering chamber is seen below. From *Physics of Thin Films*[10].

The following information has been adopted from *Physics of Thin Films*[12].

As electrons are ejected from the surface of the cathode they ionize the argon,

forming a plasma. Once charged, the newly formed ions are accelerated toward

the material, also called the target. As the target is bombarded by these ions,

material is ejected in the form of neutral atoms or as ions. The argon ions, at

this point, gain back their lost electrons and are returned to the system. Given

enough time, the entire chamber and substrate become coated with the material from the target. Argon is commonly used in a sputtering system, because of its high mass and inert properties. Particles bombarding the target with a high mass will be more efficient because they will penetrate further into the material. Argon is also appealing because of its inert chemical properties, not to mention fact that it is relatively common compared to other noble gases.

It is helpful to define several equations governing cathode sputtering. Equation 2 determines the amount of material sputtered onto a surface:

$$Q = \frac{k\,V\,i}{pd} \qquad\qquad (2)$$

Where Q represents the thickness of the film, V is the voltage, i is the discharge current, p is the pressure, k is a proportionality constant, and d is the distance between the substrate and target. As the pressure increases, the mean free path of the particles is reduced and thus, the thickness is reduced. By the same token, as distance increases, the likelihood of collisions with other particles also lowers Q. The rate at which sputtering occurs differs for each material. The efficiency of the sputtering process (atoms/ion) is given by:

$$S = \frac{N_a}{N_i} \qquad\qquad (3)$$

where N_a is the number of atoms sputtered and N_i is the number of impinging ions. Equation 3 can also be written as:

$$S = 10^5 \frac{\Delta W}{i\,t\,A} \qquad\qquad (4)$$

in which ΔW is the weight lost by the target, i is the ion current, t is the sputtering

time, and A is the atomic mass of the material. In general, we can assume that heavier target materials will sputter more efficiently and will have an increased sputtering rate.

There are several problems with cathode sputtering. The working gas also strikes the surface of the substrate and embeds itself in the film. Contamination levels caused by this effect limited the usefulness of earlier cathode systems and gave rise to the modern magnetron sputtering method. By using magnetic fields to contain the plasma closer to the cathode, therefore trapping electrons near the surface of the target, higher ionization rates could be achieved.   Using these techniques a plasma can be formed at much lower pressures, which decreases the contamination

Figure 5 – A Generic DC Magnetron Sputtering System
Electrons are ejected from the surface and ionize the argon. The electrons are kept near the surface by an E and B field to increase ionization probability. From MightyMak Sputtering Sources Owners Manual [11].
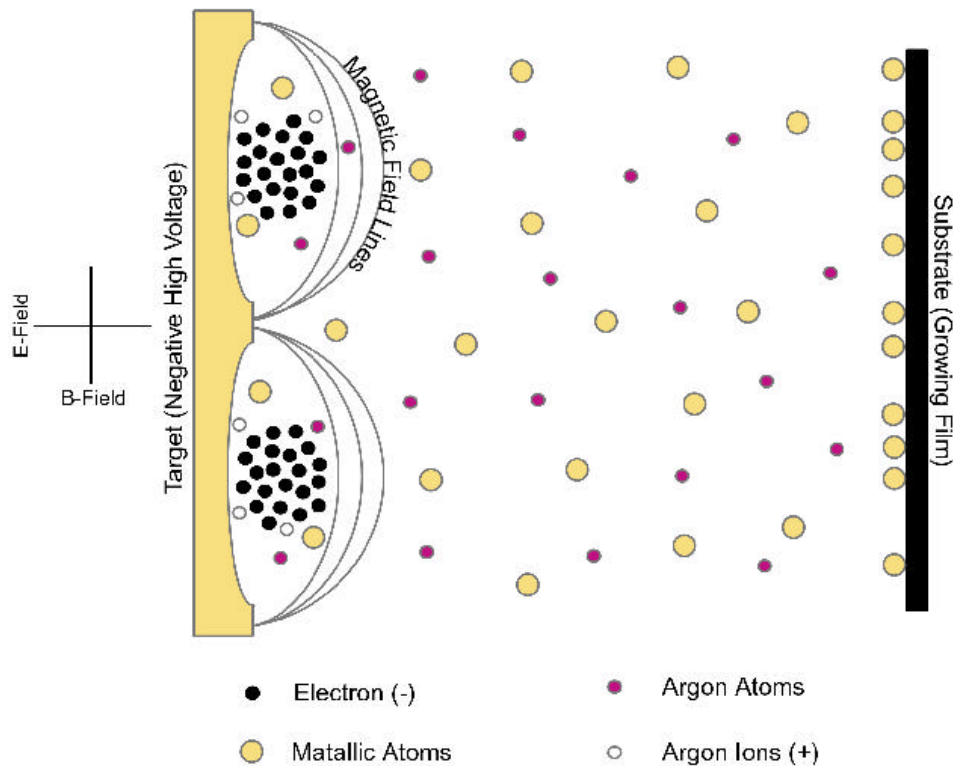
caused by argon atoms colliding with the substrate. By applying an electric field, the E X B drift currents could be made to close on themselves, which helps to hold the plasma near the target, again, increasing the likelihood of ionization. DC power sources worked fine for conductors. However, for insulators the surface becomes positively charged, which repels the bombarding ions from the cathode, halting the sputtering process. Changing the polarity with a frequency in the MHz range attracts electrons to the surface long enough to neutralize the positive charge on the cathode. Because the frequency is the same as that of radio waves, the process is known as Radio Frequency (RF) Sputtering. In our

case, only metals were deposited, so DC Magnetron Sputtering was used (See Figure 5 above).

III. Experimental Procedures

A. Growth of Thin Films

Carbon nitride (CN) may be a very promising material for use in thin film technology. One goal of these experiments is to determine what effect depositing a ferromagnetic thin film on CN might have on the magnetic properties of the ferromagnetic film. Also important is the interface between the layers of the CN and the magnetic material. If the interface is too rough it might adversely influence the GMR properties of the film. In order to construct a carbon nitride multilayer, the film must be heated during production in order to promote the growth of the film; thus, it was important to determine the effects of heat when applied to the sample.

The carbon and carbon nitride films were first deposited on silicon substrates by Jason Gammon using a separate sputtering chamber. The conditions under which these were grown are displayed in Table 1.

Table 1 – Conditions Under Which CN Films Were Grown. Three CN films were grown in all. The table lists the conditions under which they were deposited.

Sample #	Sputtering Gas	Time Sputtered (minutes)	Substrate Temperature (Celsius)	Power (W)	Current (A)	Expected Thickness (nanometers)	Deposition Rate (Angstrom per watt second)
001	Nitrogen	35	Room Temperature	98	0.152	~500	0.024
002	Nitrogen	35	300	98	0.154	~500	0.024
003	Nitrogen	35	600	98	0.15	~500	0.024

The ferromagnetic films (nickel) were grown on top of the carbon and carbon nitride films in another vacuum chamber located in Lab 325 of McGlothin-Street Hall at the College of William and Mary. This stainless steel chamber is shown in Figure 6.
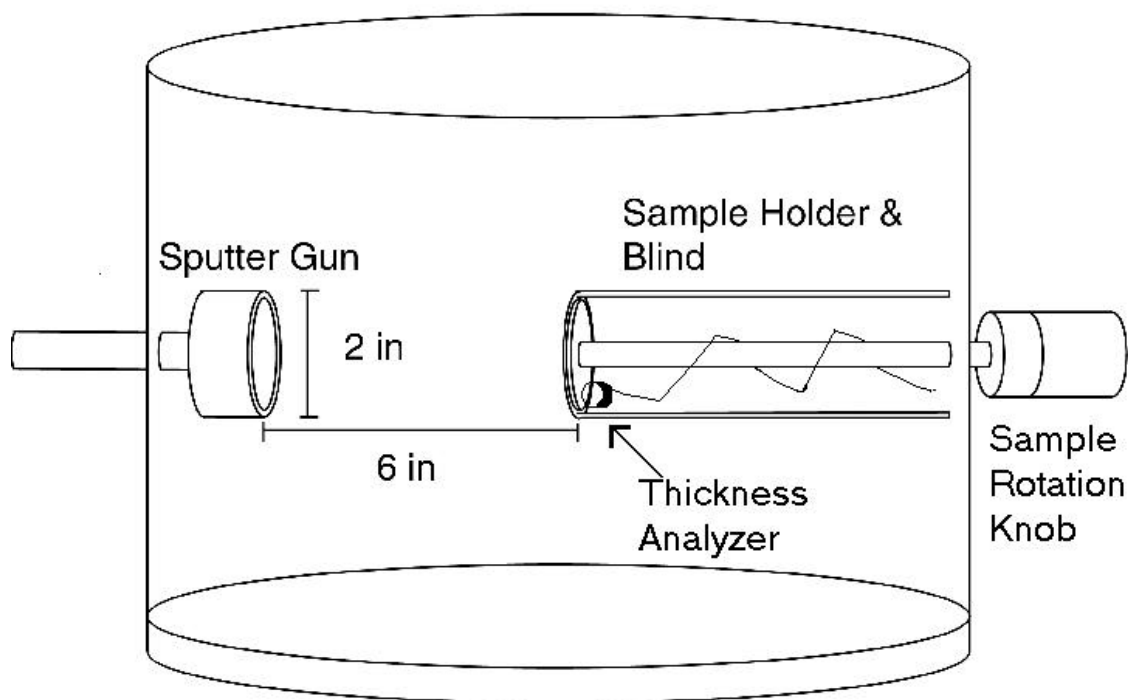

Figure 6 – The Sputtering Chamber. This is a diagram of the chamber used in our experiments.

There are several important parts to this chamber. Starting from the left is the magnetron sputter gun mentioned earlier. This particular unit is MightyMak Sputtering Source manufactured by US Inc. Because the experiment calls for the sputtering of conductive material, we used the DC method, although this unit is capable of operation in both DC and RF modes. A model MDX-1K power supply made by the Advanced Energy Corporation powered the gun. Though

higher outputs are possible, for this experiment it was unnecessary to exceed a power of 450 watts. Further to the right of Figure 6, we come to the sample holder and blind. The Sample Holder can be used to hold up to 6 samples at once.

In order to determine deposition rates a film thickness monitor was attached to position six of the sample holder. In our case, the Sycon Instruments model STM-100/MF Thickness/Rate Monitor was used for this purpose. The sample blind is a circular metal disk that can be suspended in front of the sample holder. It has one slit, which allows only one film at a time to be covered. When using the blind the sample rotation knob allows the samples to be manual rotated in front of the slit for sputtering.

The chamber is equipped with several monitors. The HPS SensaVac Series 953 Pirani/Cold Cathode Gauge System is a combination unit consisting of both a Pirani and Cold Cathode Gauge. With these two gauges and the HPS 953 Controller, which automatically switches between them depending on the pressure, it is possible to measure pressures from 10^4 to 10^{-10} Torr. The MKS 427 Flow Controller monitors the flow of argon gas into the chamber during sputtering. Finally, the Stanford Research Systems Model RGA 200 Residual Gas Analyzer measures the partial pressures of all gases in the chamber, which can also be used for leak testing. Helium is sprayed around the location of a suspected leak when the chamber is under vacuum. When the RGA detects a sharp increase in helium levels the leak has been located.

To produce films the chamber must be at relatively low pressures. In order to bring the chamber to high vacuum a Leybold Vacuum Trivac D 65 Rotary Vane Pump roughing pump first lowers the chamber pressure to the low vacuum scale. This particular pump will decrease the pressure to approximately 6×10^{-1} Torr before it becomes ineffective. This pump also removes the majority of the water vapor from the chamber. Once that has been accomplished, the pump is shut off and the Cryo-Torr 10 High-Vacuum Pump (by the Helix Technology Corporation) lowers the vacuum in the chamber further. The Cryo-Torr 10 is a type of cryogenic pump. Basically, it is a large refrigerator with liquid helium at about 4K as a refrigerant and, in our setup, uses the 8500 series compressor by the same manufacturer. When molecules of air strike the sides of the cold chamber they stick to it.

Often, we want to manufacture films that have very similar characteristics. For that purpose it might be desirable to determine the deposition rate using the film thickness monitor before depositing the first films. When not using the blind, e.g. producing films with the same thickness, the monitor can be used to give us an accurate total thickness rate in real time, as well as the deposition rate.

Our experiment used a total of six different films. Three were formed with a single layer of carbon nitride and a second layer of nickel covering the first. Two more were composed of a layer of carbon with nickel again on top. The sixth was a simple nickel film. All of the six films were deposited on silicon substrates. Four useable samples were created in all. Samples 001, 002, and

003 were all given a layer of carbon nitride at varying substrate temperatures. Then each was covered with a second layer of nickel. The final sample was number 006 and was simply nickel on a silicon substrate. This sample was for comparison, to determine if the carbon nitride or carbon layer had any affect at all on the properties of the nickel films. Two carbon films were also produced (004 and 005), but their quality was too poor to be used in the study. After data collection, each sample was annealed for 6 hours in a 200°C oven surrounded by inert argon gas to avoid formation of nickel oxide. The films were then reexamined.

B. Measuring Thickness and Roughness of the Films

Graph 1 – Deposition Rates as Measured by the Thickness Monitor.
The deposition rate for nickel was taken using a film thickness monitor and plotted.
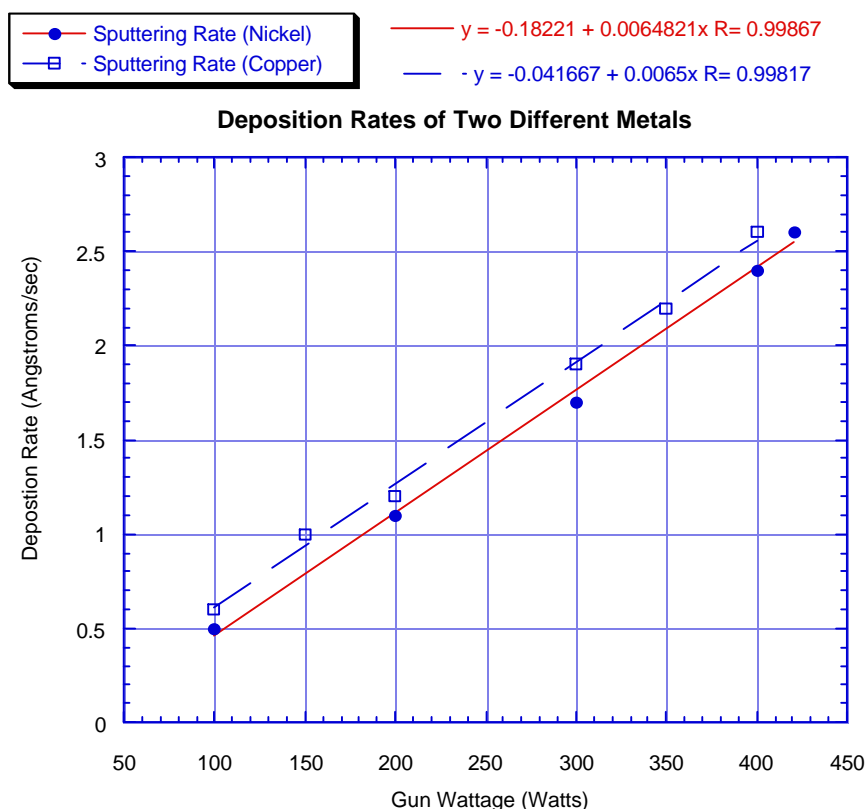
Power (Watts)

Using the thickness monitor, we determined the deposition rate of the nickel (Graph 1 above). The results varied linearly with gun power. (Notice the difference in sputtering rates between the heavier and lighter materials).

It was impossible to measure the deposition rate for the carbon while it was being deposited. Therefore, a Dektak Surface Analyzer had, located at the Applied Research Center located in Newport News, Virginia, was used to measure thickness. The computer-controlled Dektak runs a small needle across the sample detecting any difference in height as the head moves up and down. That data is summarized in Table 2 below.   Dektak data for nickel is also presented here as a comparison between the information given by the film thickness monitor. The data has been presented as the deposition rate per watt (the same units as the slope of Graph 1) to make up for the fact that the samples were grown at different sputtering powers.   The Dektak estimates are 18% higher for nickel than the same numbers recorded from the monitor.

Table 2—Depostion Rate As Measured By Dektak Surface Analyzer.
Because we were unable to measure the thickness of the CN layers deposited a Dektak Surface Analyzer was used. Nickel and copper data is provided for comparison. Resolution of the Dektak is about 10 Angstroms

Material	Deposition Rate per Watt as Measured by Dektak (Angstroms/Watt*Second)	Deposition Rate per Watt as Measured by Thickness Monitor (Angstroms/Watt*Second)
Nickel	0.00766	0.00648
Carbon	0.024	Not Available
Carbon Nitride	0.024	Not Available

Table 3: Nickel Deposition Parameters A layer of nickel of deposited over the three CN films under the conditions below. Sample 006 is simply nickel on silicion. (Resolution for the Deposition Monitor is about 0.1 angstroms/second)

Sample #	Sputtering Duration (minutes)	Power (Watts)	Deposition Rate (Angstroms / second)	Thickness Of Nickel Layer (Angstroms)
001	10	200	1.1	660
002	10	200	1.1	660
005	10	200	1.1	660
006	10	200	1.1	660

The four samples (three nickel films on CN and one nickel film on silicon) were taken to the NASA Langley Research Center for further testing. To determine the roughness a technique called Atomic Force Microscopy (AFM), also known as Scanning Force Microscopy was used. It measures the force between the tip of a probe and the surface being scanned. The probe is attached to a cantilever beam with a spring constant of about 0.1 – 1.0 N/m. This number is at least one order of magnitude lower than the spring constant of an average atom. A laser beam is directed at the tip and a photosensor detects changes in its reflection as it moves across the surface of the sample. Valuable information about surface topology as well as calculations of average roughness, root-mean-square roughness, and the Z range (range of heights) can all be made by the AFM.

The two most commonly used methods for measuring surface roughness are average roughness (RA) and root-mean-square roughness (RMS). Average

roughness is defined as:

$$RA = (1/N) \sum_{i=1}^{N} |z_i - z_{avg}| \tag{5}$$

where N is the total number of measurements, z_i is the height at a point i, and z_{avg} is the average of all measurements. Average roughness is nothing more than the mean deviation of the height measurements. Root-mean-square roughness is the standard deviation and is give by the familiar formula in equation 6:

$$RMS = [(1/N) \sum_{i=1}^{N} (z_i - z_{avg})^2]^{1/2} \tag{6}$$

Roughness measurements were made for each film before and after annealing. These results are listed in Table 4 in the Results section.

C. Vibrating Sample Magnetometry

Before the annealing process took place, a Lakeshore 7300 Vibrating Sample Magnetometer (VSM) was used to record the hysteresis loops for each film. This VSM is also located at the NASA Langley Research Center. The large electromagnet in the VSM produces a magnetic field around a sample, which creates a magnetization in the film. Then, it is allowed to vibrate in a sinusoidal manner. The changes in flux caused by the vibrations are translated into a change in current in the pickup coils of the instrument, which registers as

a particular magnetization of the film. With a sensitivity of 10^{-5} emu the VSM gives an accurate measurement of the magnetization. The largest source of error in this measurement is the difficult process of aligning the films between the pickup coils which causes the hysteresis loops to shift up or down from zero. Minimal effort is required to correct the problem in the data.

IV. Results

A. Roughness of Flims

The AFM at NASA Langley Research Center took the scans in Table 4. The results for mean and RMS roughness are summarized there.

Table 4 – Results of the AFM Scans Prior and After Annealing
(All the samples were annealed for six hours at 200 degrees C. Before annealing Z range, RMS, and RA data was taken)

Sample	Description	Z Range (nm)	RMS (nm)	RA (nm)
001 before annealing	Nickel on CN at room temperature	26.736	3.157	2.509
001 after annealing	Nickel on CN at room temperature	51.195	12.910	3.140
002 before annealing	Nickel on CN at 300 Degrees C.	42.540	4.985	3.819
002 after annealing	Nickel on CN at 300 Degrees C.	61.924	7.847	5.632
003 before annealing	Nickel on CN at 600 Degrees C.	51.371	6.337	4.956
003 after annealing	Nickel on CN at 600 Degrees C.	63.649	5.356	3.721
006 before annealing	Nickel on silicon	15.479	1.263	1.000
006 after annealing	Nickel on silicon	59.659	7.232	5.305

The following scans were taken by an AFM at the NASA Langley Research Center. First we scanned the films prior to and after annealing. (See Figures 7 to 10)

Figure 7 – Nickel on CN deposited at room temperature. Before and After Annealing (Notice the islands of nickel forming after the film has been annealed.)
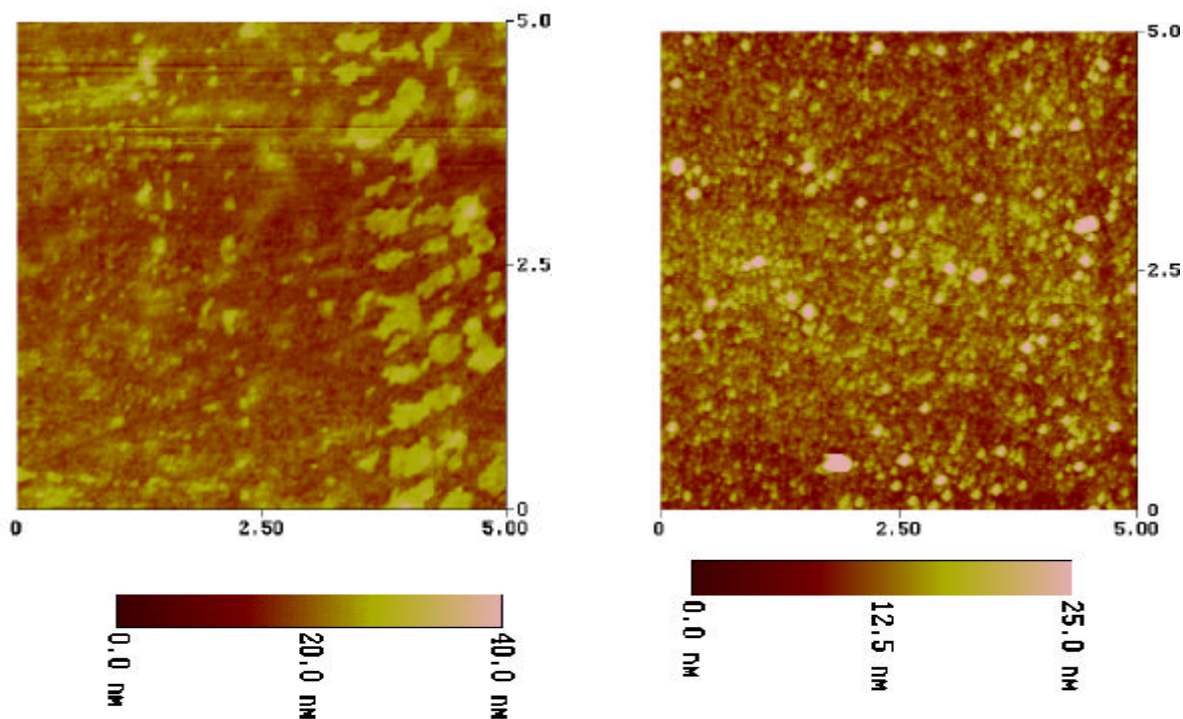
Characteristic of most of these scans we note before annealing, the nickel forms large islands over the CN. Then, afterward, it forms together creating specs of nickel all over the film. Material is obviously clumping together on the surface, since Z is much higher for the annealed data. For the case of nickel grown on the CN deposited at room temperature, the film is greatly affected by annealing (the change in RMS roughness is almost 10 nm). It too forms large islands. For nickel on CN deposited at higher temperatures, RMS roughness

appears to be only slightly affected by the annealing process. In fact, changes

between the RMS values prior to and after annealing only vary by around 3 nm.

It could be the nickel simply adheres better to the presumably more stable

carbon nitride. Also, the carbon nitride films appear to withstand annealing

better when deposited at higher substrate temperatures.

Figure 8 – Nickel on CN Deposited at 300 degrees. Before and After Annealing (The dark colors show us an increase in Z range, characteristics of all the films tested. Notice that the "islanding" is lesser on the presumably harder CN.
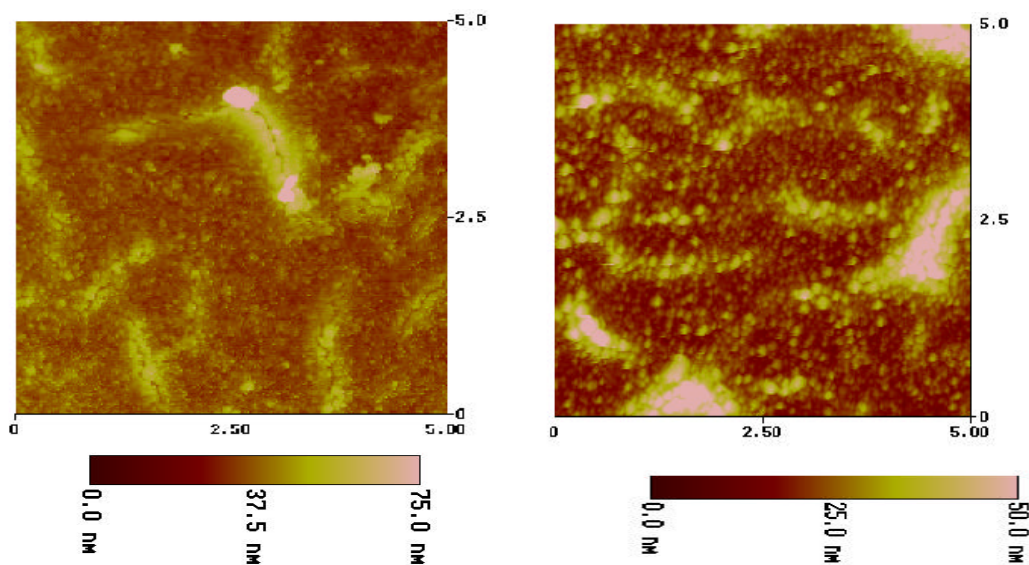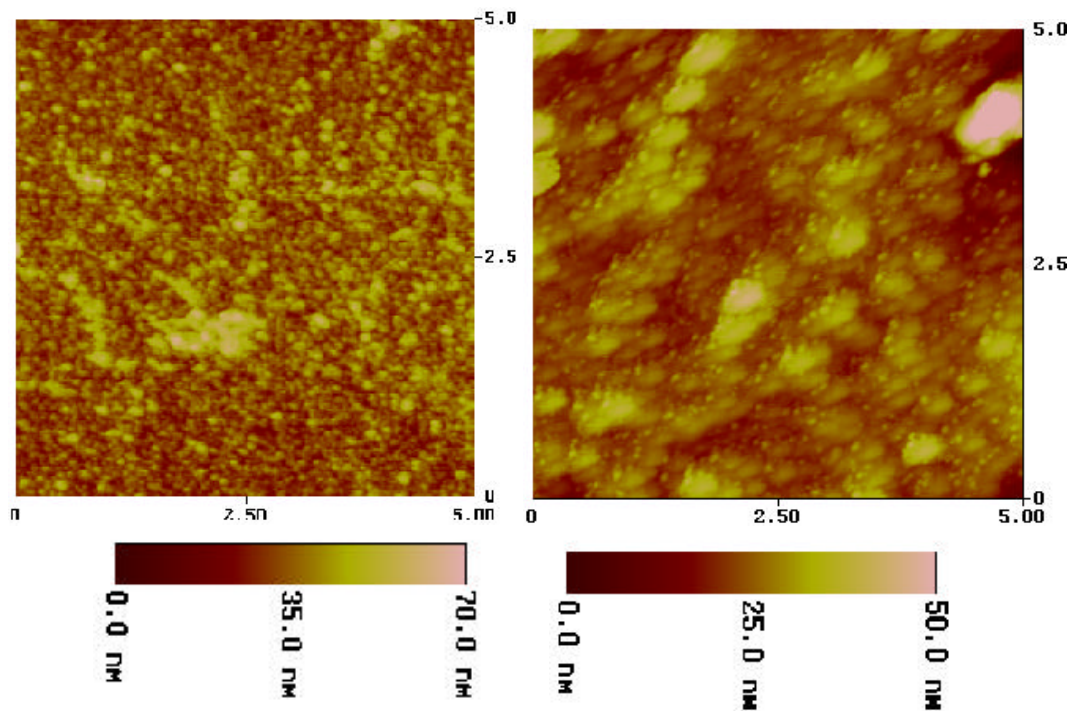
Figure 9 – Nickel on CN Deposited at 600 degrees. Before and After Annealing. Z range does not increase nearly as much. Also, the film has become a little smoother.

RMA and RMS roughness for this film showed no large variations as compared to sample 001. In fact, unlike films 001 and 002, Sample 003 showed a slight decrease in RMS roughness. Although the nickel is much less ordered, which might affect magnetic characteristics, the surface held up much better to high temperature.

Figure 10 – Nickel on Silicon. Before and After Annealing (Nickel on silicon shows the most dramatic change. The islanding effect is greater. Z range becomes very high also.)
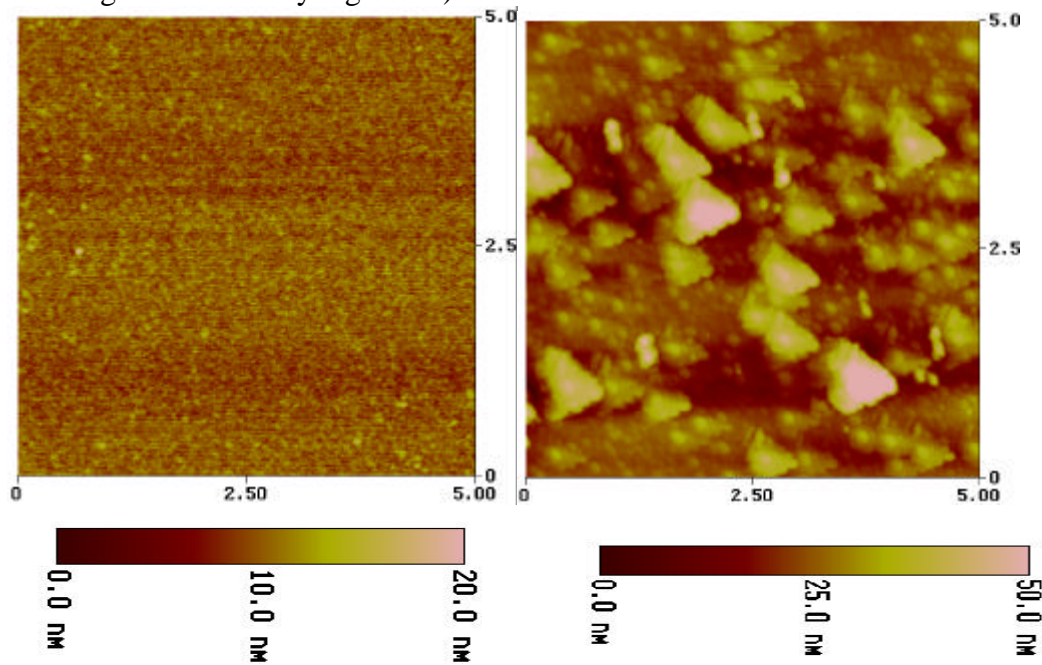
The plain nickel film on silicon was grown as a comparison to the CN films. By far the smoothest surface starting out, it had the largest change in Z. After annealing, both the RMS and RMA roughness values are higher than those taken from sample 001 are. It can be inferred that a well made CN / Ni film can, and does, fair better under heating than the nickel on silicon film.

In all of these films we saw nickel forming together in relatively large islands of material. Three possible explanations for this are nickel forming on the surface, the possible intermixing of the layers, and / or perhaps even the forming of nickel carbides during annealing. It should be noted that it was very difficult to produce an inert environment in our oven. Therefore, it could be that nickel oxide might have formed on the films, which could have caused some of

the changes we see in the figures displayed.

B. Magnetic Properties

Hysteresis loops were taken for all films prior to annealing using the VSM. That data appears below in Graphs 2, 3, and 4. However, only some of the films were scanned after being annealed. The surface of many of the annealed films became so easily damaged from even simple handling that a large portion lost a considerable amount of their nickel layer. The data that was taken showed very poor results. It is almost without a doubt that these poor numbers were caused by contamination of the films during annealing. Particularly, the nickel could have reacted with oxygen to form nickel oxide, which has the potential to ruin the magnetic properties of the films. The data for magnetic properties of the annealed films is not shown.

Graph 2 – Hysteresis Loops for Films Prior to Annealing.

Sample 001 showed a saturation magnetization. Samples 002 and 003 were very much like Nickel on Silicon, Sample 006
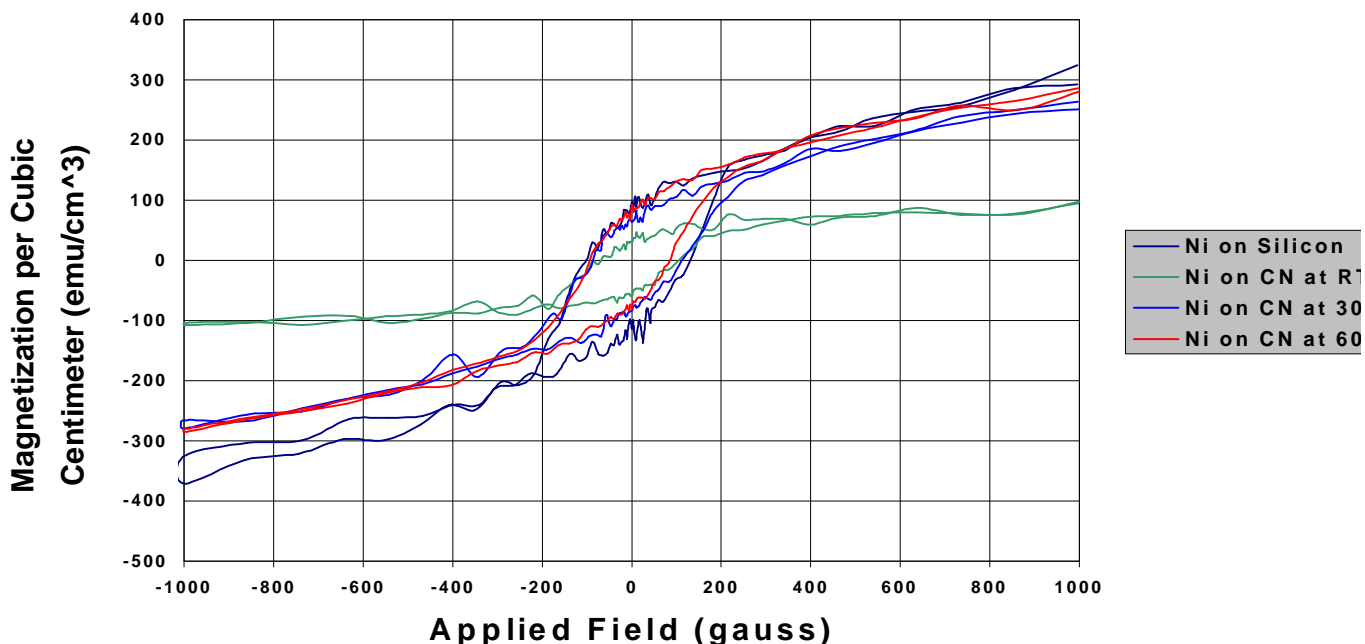
Notice how saturation magnetization increases dramatically in Samples 002 and 003 when compared to nickel on CN deposited at room temperature. The nickel film *and* the two samples deposited at higher substrate temperatures have a saturation magnetization of approximately 300 emu/cm^3 measured at 1000 Gauss. Nickel deposited on CN at room temperature is as low 100 em/ cm^3. The maximum expected magnetization of nickel is 470 emu/cm^3. This fact gives weight to the argument that CN could be incorporated into various multilayer films, if manufactured properly. By studying Graph 3 (below) we also realize that there is a substrate temperature where saturation magnetization is maximized. Or, it might be that at substrate temperatures higher than 600°C, we see little change.

Graph 3 – Substrate Temperature as Related to the Saturation Magnetization. Sample 003, grown at the highest substrate temperature, shows more favorable saturation magnetization levels then the other CN / Ni films
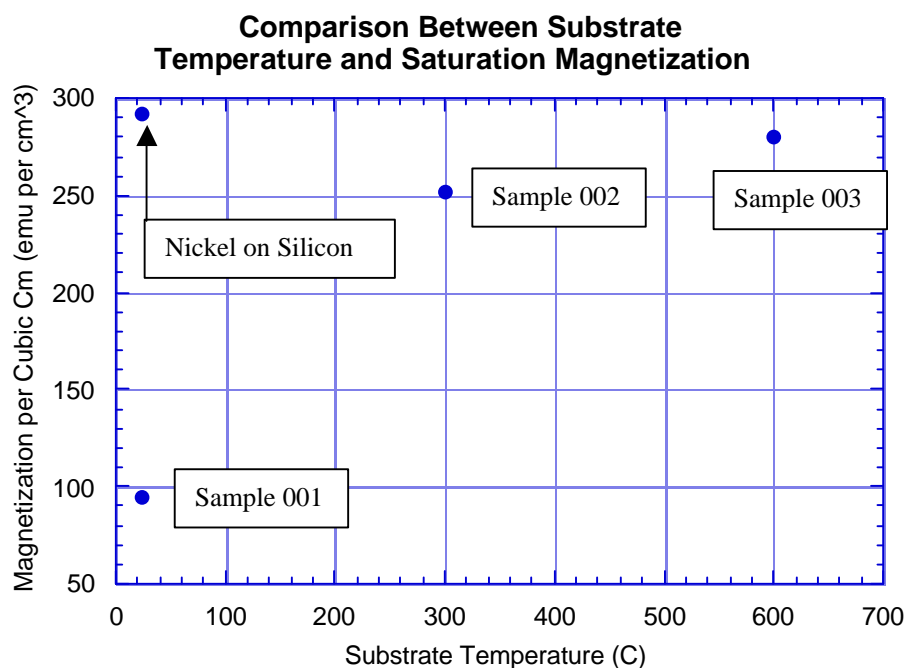
When interpreting a hysteresis loop, we should consider not only saturation magnetization, but also coercivity. The coercivity of the film is a measure of how sensitive the response to a magnetic field is. Saturation magnetization, on the other hand, measures the responsiveness to the applied field. The best films for use in GMR materials should exhibit the lowest possible coercivity and highest saturation magnetization. Graph 4, below, shows the relative coercivities of the samples.

Graph 4 – The Coercivities of the Films. For Ni / CN grown at 600 degrees C, we see very little change in coercivity from the Ni on silicon film.

VSM Curves Prior to Annealing
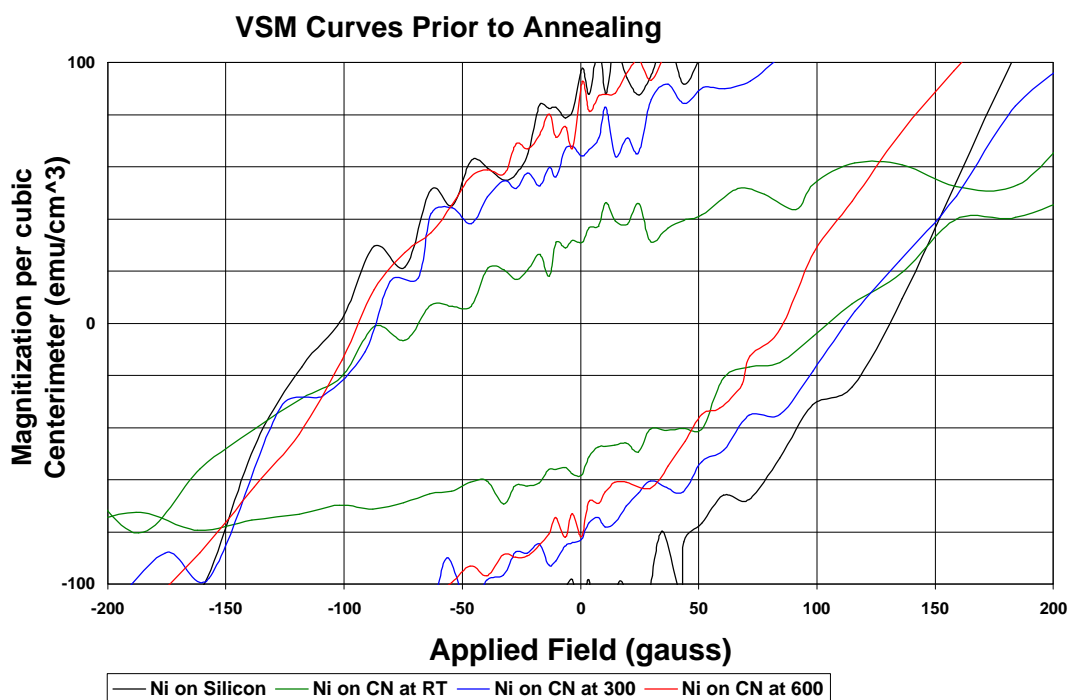
The coercivity decreases for our Ni / CN films, but this change cannot be called significant. Although the addition of the CN seems to affect the magnetic properties of the film only slightly, it is important that it is, in fact, lower than the

pure nickel film. Also notice that there is a shift in the curves slightly to the right of center. The shift could be due to the formation of nickel oxide on the surface of the film, which pins the magnetization in a specific direction.

V. Conclusion

Preliminary data suggests that carbon nitride might be a good candidate for use as an insulating layer in films exhibiting the GMR effect. The AFM scans taken show that while the nickel films on CN are much rougher than nickel on bare silicon, they are more resistant to islanding when heated. These scans revealed that the Ni / CN films exhibited a lesser islanding effect and a lesser increase in surface roughness over nickel on silicon. In terms of the research, nickel is an appropriate metal to use. In fact, most industrial applications use permalloy, a mixture of 80% nickel and 20% iron, as conductive layers in GMR devices. Our data supports the fact that the interface between CN and nickel can be made relatively smoothly and uniformly. Furthermore, we now know more about the production of CN films. From the annealing data, it appears that the material will stand up well to heating, which would be required if a multilayer using carbon nitride was produced. Also, there definitely is a maximum substrate temperature at which these films exhibit optimum performance. We also know that as temperature increases the changes are either less pronounced or perhaps even detrimental to our purpose. The magnetic properties of the GMR effect are also linked to substrate temperature and the idea that there exists an optimum growth temperature. Both saturation

magnetization and coercivity in the best performing samples of the CN / Ni films (Samples 002 and 003) were comparable to those found on the pure nickel film.

Carbon nitride looks to be an acceptable choice for use in GMR studies, further experimentation is certainly warranted in this area of research. The next step should be to create a multilayer example and test its properties when annealed and grown under varying temperatures as in the experiment. Data must also be taken after annealing by using the VSM, or other similar process, simply to ensure that magnetic properties hold after the film is subjected to heat. Studying the AFM scans, the possibility to produce better results might be increased by using more careful annealing methods. Time and energy is clearly well spent in these pursuits.

References

[1] Gary A. Prinz, "Spin-Polarized Transport," Phys. Today, 58 (April 1995)

[2] Gary A. Prinz, "Spin-Polarized Transport," Phys. Today, 58 (April 1995)

[3] From IBM Research *www.research.ibm.com/journal/rd/421/parkin.html, www.reaserch.ibm.com/journal/rd/421/nesbet.html*, December 2000

[4] Faltin, Heather A. *The Magnetic and Electrical Properties of Permalloy-Carbon Thin Film Multilayers*. (William and Mary College, April 2000).

[5] John L. Simonds, "Magnetoelectronics Today and Tomorrow," Phys. Today, 26 (April 1995)

[6] Anne Reilly, College of William and Mary, Unpublished Grant Proposal

[7] David J. Griffiths. *Introduction to Electrodynamics*, (Upper Saddle River, New Jersey 07458: Prentice Hall, 1999), Chapter 5.

[8] Neil W. Ashcroft, *Solid Sate Physics* (New York: Holt, Rinehart and Winston, 1976)

[9] W. K. Liu, M. B. Santos, *Thin Films: Heteroepitaxial Systems*, (Singapore: World Scientific Publishing Co. Pte. Ltd, 1999), 141.

[10] Ludmila Eckertova, *Physics of Thin Films*, (New York: Plenum Press, 1986), 46-54.

[11] *MightyMak Sputtering Sources Owners Manual Manufactured by US Inc.* US Inc. San Jose, CA 95119-1365.

[12] Ludmila Eckertova, *Physics of Thin Films*, (New York: Plenum Press, 1986), 46-54.

[13] C. Richard Brundle, Charles A. Evans and Shuan Wilson, *Encyclopedia of Materials Characterization*. (Boston: Butterworth-Heinemann, 1992). Chapter 14.